

Indirect Learning DPD: Analytical Framework and Closed Form Solution

Ramez Moh. Elaskary*, Ahmed Hesham Mehana[§], Yasmine Fahmy[§], and Mona El-Ghoneimy[§]

*Department of Electronics and Electrical Communications Engineering, Institute of Aviation Engineering and Technology, Giza, Egypt

[§]Department of Electronics and Electrical Communications Engineering, Cairo University, Egypt

Email: ramez.moh.elaskary@gmail.com, ahesham@iecc.org, yasfahmy@hotmail.com, melghoneimy@yahoo.com

Abstract—The baseband digital predistortion (DPD) signal processing technique is an effective way to compensate the nonlinearity effect of the power amplifier. Because of, the lack of analytical closed form estimate for the DPD coefficients, this problem stands as an impenetrable barrier in the way of a lot of researches to complete the mathematical model of their systems. In this paper, we analyze the indirect learning architecture (ILA) and derive a closed form expression for the DPD coefficients analytically, which is the first of its kind. Moreover, without loss of generality, we introduce a simple analytical case study at a specific memory depth and a nonlinearity order of the power amplifier (PA), to facilitate the presentation of mathematical relationships, so that we apply the analytical framework of DPD coefficients on it. Furthermore, a performance comparison between the DPD using the derived coefficients and the DPD using Monte Carlo simulation is obtained, the performance comparison shows that the derived DPD coefficients relationships are valid. Finally, we provide approximate relationships of the DPD coefficients closed form, the approximate relationships appear adequate, through simulations, up to a certain input power.

I. INTRODUCTION

To meet the exponential growing demand of subscribers for higher data rates, capacity, reliability, and new services, modern wireless communication devices have to evolve to exploit the available spectrum band and network resources more efficiently. In other words, the most two important points in developing of the wireless communication systems are energy and spectral efficiencies enhancements. Indeed, Massive Multiple-input multiple-output (MIMO) was subject to intensive research within the last few years since it can greatly improve the spectral efficiency [1]-[3], as well as the energy efficiency [4], [5]. The Massive MIMO system scales up MIMO by deploying a large number of base station antennas, usually much larger than the number of users [6].

One of the main challenges in massive MIMO systems is the large number of radio-frequency (RF) chains that include non-linear power-hungry amplifiers. Generally, a nonlinear device produces intermodulation distortion (IMD) to the transmitted signal band which causes spectral regrowth [7], [8]. Thus, to reduce the unwanted emissions, the transmit power has to be reduced such that the power amplifier (PA) operates in the linear region; however, this leads to a decrease in the PA efficiency (energy inefficient) and possible decrease in the network coverage, thus this is an impractical solution. Subsequently, the PA linearization play a crucial role to improve the PA efficiency. PA linearization techniques include

analog feedback linearization, feedforward linearization, RF predistortion, and baseband digital predistortion (DPD) [9], [10].

Among all linearization techniques, the DPD is the most cost efficient as it is digitally implemented on the baseband processor and can be reconfigurable when needed. In this paper, we analyze the performance of DPD in OFDM system. Polynomial-based modeling for the PA and DPD is commonly used because of its low complexity (compared to other approaches, such as neural network) and good performance [11]. Generally, any DPD architecture can be divided into two paths, the first one is the DPD processing path (also called actuator) and the second is the DPD training path that updates the DPD coefficients in the main path. The DPD main processing path is simply applying a nonlinear function at the input of the PA which is almost inverse of the PA nonlinear response, such that the overall of the two subsystems (DPD and PA) is linear. DPD training path can be built in four different architectures: direct learning architecture (DLA), indirect learning architecture (ILA), iterative learning control (ILC) architecture, and closed loop learning architecture. In this paper, we consider the ILA mode as it is commonly used [12]-[15]. ILA approach exploits the theory mentioned in [16], [17] that uses the P^{th} -order inverse of Volterra nonlinearities, and estimates the postdistorter by minimizing the error between the postdistorter output and the PA input signal. Then, this postdistorter is used as a predistorter assuming that they are equivalent.

In this paper, we analyze the ILA DPD model and analytically obtain the DPD coefficients in closed form. To the best of our knowledge, this is the first work that derives closed-form values for the coefficients for polynomial-based DPD model. This can help providing mathematical model and quick comparison between different systems and different specification for the DPD. the contributions can be summarized as

- We obtain analytical closed form expression for the ILA DPD coefficients.
- We provide a case study and a performance comparison between the DPD using the derived coefficients and the DPD using Monte Carlo simulation.
- The approximate relationships of the DPD coefficients closed form and performance comparison are obtained.

The rest of the paper is organized as follows: in Section II, the OFDM signal model, nonlinear PA model, and ILA are shortly introduced. Then, in Section III, the proposed analytically DPD coefficients calculations is introduced and

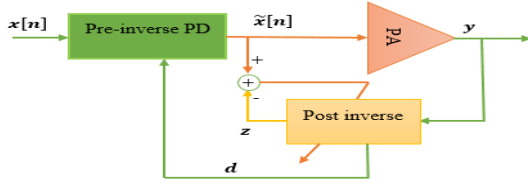


Figure 1. Schematic diagram of ILA

described. Section IV analyzes the proposed DPD algorithm for certain memory depth and nonlinearity order of the PA. Section V provides the numerical results and the approximate relationships of the DPD coefficients. The concluding remarks are given in Section VI.

Notation: For a matrix \mathbf{Y} , we use \mathbf{Y}^T and \mathbf{Y}^H to denote the transpose and the conjugate transpose of a matrix \mathbf{Y} , respectively. Also, the symbol $|x|$ indicates the absolute value of x . Moreover, $E[\cdot]$ and $Var[\cdot]$ denotes the expectation and the variance operators, respectively.

II. SYSTEM MODEL

A. OFDM signal model

The equivalent low-pass OFDM symbol with N sub-carriers and appended with guard interval of length N_g samples is expressed as

$$\tilde{x}[n] = \frac{1}{N} \sum_{k=0}^{N-1} b_k e^{j2\pi nk/N}, \quad -N_g \leq n \leq N-1 \quad (1)$$

where $\tilde{x}[n]$ is the PA input sample at time index n , b_k is the complex data OFDM symbol of k^{th} subcarrier. b_k 's are independent and identically distributed (i.i.d.) with zero mean and variance P_a . When N is large enough, $\tilde{x}[n]$ can be assumed, by central limit theorem, to be a complex Gaussian process that expressed as

$$\tilde{x}[n] = u[n] + jv[n] \quad (2)$$

where $j = \sqrt{-1}$, u and v are Gaussian processes with zero mean and variance σ^2 [18], [19], i.e. \tilde{x} is complex Gaussian process with zero mean and variance $\frac{P_a}{N} = 2\sigma^2$.

B. Nonlinear PA model

There are various models that describe the PA behavior, which include the Volterra series, the Wiener model, the Hammerstein model, and the Wiener-Hammerstein model. The memory polynomial behavioral model (Volterra series) is proposed in [20] as the following:

$$y[n] = \sum_{k=0}^{K-1} \sum_{m=0}^{M-1} a_{k,m} \tilde{x}[n-m] |\tilde{x}[n-m]|^k \quad (3)$$

where \tilde{x} is the baseband PA input signal and is equal to x in the start, y is the PA output, $a_{k,m}$ are the PA coefficients, M is the PA memory depth, and K is the PA nonlinearity order.

C. Indirect learning architecture (ILA)

ILA will be presented to construct the predistorter for the nonlinear PA. The conventional ILA model is shown in figure 1. As previously stated, the post-inverse model of PA is determined first, therefore used as a predistorter before the PA i.e the postdistorter and predistorter are identical [16], [17]. Thus, the main task is determining the postdistorter coefficients such that the overall system (DPD+PA) is linear. Hence, to model the nonlinear post inverse, replace the roles of y with z and \tilde{x} with y in equation (3) as the following:

$$z[n] = \sum_{k=0}^{K-1} \sum_{m=0}^{M-1} d_{k,m} y[n-m] |y[n-m]|^k \quad (4)$$

where $d_{k,m}$ is the DPD coefficients is chosen such that $z[n]$ is closest to the input signal $x[n]$. Thus equation (4) can be rewritten as a set of system of linear equations in a matrix form as the following:

$$\mathbf{z} = \mathbf{Y}\mathbf{d} \quad (5)$$

where \mathbf{z} , \mathbf{d} , and \mathbf{Y} are obtained in equations (6) and (7), respectively. Equation (7) is in the beginning of the next page

$$\mathbf{z} = \begin{bmatrix} z[n] \\ z[n+1] \\ \vdots \\ z[n+L-1] \end{bmatrix}, \quad \mathbf{d} = \begin{bmatrix} d_{0,0} \\ d_{0,1} \\ \vdots \\ d_{K-1,M-1} \end{bmatrix} \quad (6)$$

Where L is the number of training symbols (observations) that are used to calculate the DPD coefficients. Therefore, the DPD coefficients can be expressed from equation (5) as:

$$\mathbf{d} = [\mathbf{Y}^H \mathbf{Y}]^{-1} \mathbf{Y}^H \mathbf{z} \quad (8)$$

In order to compute the DPD coefficient, numerical calculation through Monte Carlo simulations are commonly used. This is because there is no closed form mathematical model for the DPD coefficients. In this section, we provide an analytical framework to compute these coefficients which can be easily plugged in different system models for performance evaluation. Simulation results verify the accuracy of our approach.

The method is simply divided into three steps: 1) compute $\mathbf{Y}^H \mathbf{Y}$ and its inverse, then 2) calculate $\mathbf{Y}^H \mathbf{z}$, and 3) finally multiplying them; we are exploiting the Gaussianity property of the multiple added sinusoids (OFDM signal) that are input to non-linear amplifier.

III. DPD COEFFICIENTS ESTIMATION

In this paper, we introduce a new insight to existing works that calculates the DPD coefficients $d_{k,m}$, such that $d_{k,m}$ are function of the PA coefficients $a_{k,m}$ and signal power σ^2 .

From (6) and (7), after some mathematical manipulations, assuming large training symbols ($L \rightarrow \infty$) we can write $\mathbf{Y}^H \mathbf{Y}$ as in (9) in the top of the next page, where

$$g_{1,K \times M} = y^*[n] y[n - (M-1)] |y[n - (M-1)]|^{K-1} \\ g_{2,K \times M} = y^*[n-1] y[n - (M-1)] |y[n - (M-1)]|^{K-1}$$

$$\mathbf{Y} = \begin{bmatrix} y[n] & y[n-1] & \cdots & y[n-M+1] | y[n-M+1] |^{K-1} \\ y[n+1] & y[n+1-1] & \cdots & y[n+1-M+1] | y[n+1-M+1] |^{K-1} \\ \vdots & \vdots & \vdots & \vdots \\ y[n+L-1] & y[n+L-2] & \cdots & y[n+L-M] | y[n+L-M] |^{K-1} \end{bmatrix} \quad (7)$$

$$\mathbf{Y}^H \mathbf{Y} = L \begin{bmatrix} E[|y|^2] & E[y^*[n]y[n-1]] & \cdots & E[g_{1,K \times M}] \\ E[y^*[n-1]y[n]] & E[|y|^2] & \cdots & E[g_{2,K \times M}] \\ \vdots & \vdots & \ddots & \vdots \\ E[g_{1,K \times M}^*] & E[g_{2,K \times M}^*] & \cdots & E[|y|^{2K}] \end{bmatrix} \quad (9)$$

For more details about equation (9), please refer to Appendix A. Also, in Appendix A, $\mathbf{Y}^H \mathbf{z} = L \mathbf{p}(n)$ is shown, where $\mathbf{p}(n)$ is a $KM \times 1$ vector at time index n that its element $p^{m,k}(n)$ is the $((m+1) + (k \times M))^{th}$ element in the vector given by:

$$p^{m,k}(n) = E[z[n]y^*[n-m] | y[n-m] |^k] \quad (10)$$

The PA model only contains odd order terms since these are the terms that mostly contribute in the IMD. The post inverse only contains odd order terms.

A. A case study

For illustration purpose, we assume a simple case study, without loss of generality, to facilitate the presentation of mathematical relationships. General form will be the follow. Let's assume $K = 3$, $M = 1$. By substituting in equation (3) hence

$$y[n] = a_{0,0}\tilde{x}[n] + a_{2,0}\tilde{x}[n] | \tilde{x}[n] |^2 \quad (11)$$

Initially, $\mathbf{d} = [1 \ 0 \ 0]^T$, hence $x[n] = \tilde{x}[n]$. By substituting in equations (9), (10), therefore

$$\mathbf{Y}^H \mathbf{Y} = L \begin{bmatrix} E[|y|^2] & E[|y|^4] \\ E[|y|^4] & E[|y|^6] \end{bmatrix} \quad (12)$$

and

$$\mathbf{Y}^H \mathbf{z} = LE \begin{bmatrix} z[n]y^*[n] & z[n]y^*[n] | y[n] |^2 \end{bmatrix}^T \quad (13)$$

thus, from (8)

$$\mathbf{d} = \begin{bmatrix} A/C & 0 & B/C \end{bmatrix}^T \quad (14)$$

where A , B , and C are obtained in the following equation.

$$\begin{aligned} A &= \sum_{k=0}^7 \alpha_k * a_{0,0}^{7-k} * a_{2,0}^k * \sigma^{2k} \\ B &= - \sum_{k=0}^4 \beta_k * a_0^{4-k} * a_2^{k+1} * \sigma^{2k} \\ C &= \sum_{k=0}^8 \gamma_k * a_{0,0}^{8-k} * a_{2,0}^k * \sigma^{2k} \end{aligned} \quad (15)$$

where α_k , β_k , and γ_k are in table I. We omit the detailed proof for space limitation. Please refer to Appendix B.

IV. PROPOSED DPD COEFFICIENTS LEARNING RESULTS

The results in this section consider two PA cases with third order nonlinear equation(11): the first PA with coefficients $a_{0,0} = 1$, $a_{2,0} = -0.4$ and the second PA with coefficients $a_{0,0} = 1$, $a_{2,0} = -0.8$, noise variance -30 dBm, and saturation point is 0.5509 V (24.8 dBm). The data length = 200 Kdata symbols and the training length = 2048 symbols. The specifications of the OFDM signal are: FFT length $N_{FFT} = 4096$, sub-carreir spacing is 120 KHz, Number of sub-carreirs in the resource block (RB) is 12, sampling frequency = 491.52 MHz, Modulation order = 256.

A. DPD performance metric

As performance metrics, we consider error vector magnitude (EVM) to quantify the in-band quality, as defined in [21],

$$EVM \% = \sqrt{P_e/P_r} \times 100 \% \quad (16)$$

where P_e is the error signal power (difference between the ideal symbol values and the corresponding symbol at the PA output), both normalized to the same average power, and P_r is the reference power of the ideal symbol constellation.

B. DPD performance results

In this section, a performance comparison between the DPD base on the conventional DPD coefficients estimation that obtained in (8) and the DPD based on the proposed analytical DPD coefficients estimation closed forms that obtained in (14).

Figure 2 shows the EVM versus the output signal power in dBm. Note that the nonlinearity effect is more pronounced in the second PA ($a_{2,0} = -0.8$). It is also shown that both the analytical and simulated DPD cases have similar performance. Moreover, we can note that when the power increases the nonlinearity effect of the PA increases and the DPD is not able to compensate the distortion above a certain limit; in this example the power levels beyond which the DPD cannot invert the PA operation are 20.5 dBm for the first PA ($a_{2,0} = -0.4$) and 19 dBm for the second PA ($a_{2,0} = -0.8$). As well as, in the figure, it is clear at low power region with increasing the power, the performance improves due to the increase of SNR, because of the performance limited by the noise in this region, but this does not long forever. As the power increases, the nonlinearity effect of the PA increases, which becomes the dominant impact on performance.

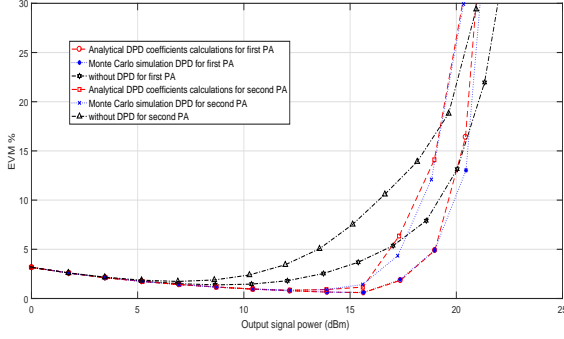
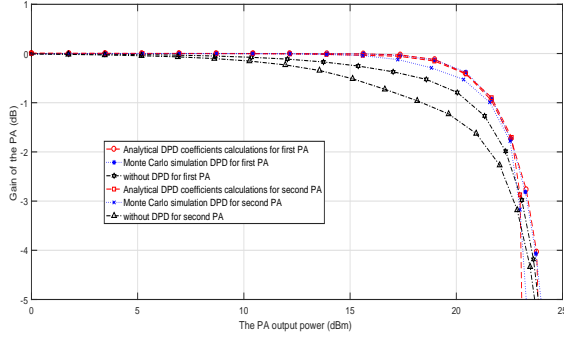
Figure 2. *EVM %* vs. output signal power in dBm for two PA's

Figure 3. The normalized gain of the PA in dB vs. output power in dBm

For the two power amplifiers that are considered, figure 3 depicts the normalized gain of the PA in dB versus the PA output power in dBm. The figure illustrates three cases, the first one for PA only, the second for the DPD using Monte Carlo simulation followed by the PA, and the third for the DPD using the derived coefficients followed by the PA. It appears the DPD based on the proposed analytical DPD coefficients estimation approach achieves approximately the same performance as the DPD based on the conventional DPD coefficients estimation.

For simplicity purposes of mathematical relationships, we can approximate the mathematical relationships of the DPD coefficients that are in equation (14), when the input power is limited. Thus, the higher order terms in equation (15) can be neglected. Therefore, the equation (15) can be rewritten as the following assuming $a_{2,0} \leq |-0.4|$ and the input power is less than 16 dBm:

$$\begin{aligned} A &= a_{0,0}^7 + 72 a_{0,0}^6 a_{2,0} \sigma^2 + 2448 a_{0,0}^5 a_{2,0}^2 \sigma^4 \\ B &= -(a_{0,0}^4 a_{2,0} + 36 a_{0,0}^3 a_{2,0}^2 \sigma^2) \\ C &= a_{0,0}^8 + 72 a_{0,0}^7 a_{2,0} \sigma^2 + 2520 a_{0,0}^6 a_{2,0}^2 \sigma^4 \end{aligned} \quad (17)$$

Also, we can make the same thing for the second PA or for any third order nonlinear PA with $a_{2,0} \leq |-0.8|$, thus the higher order terms in equation (15), can be ignored for the input power is less than 16 dBm. Therefore, the equation (15) can be rewritten as the following assuming $a_{2,0} \leq |-0.8|$ and

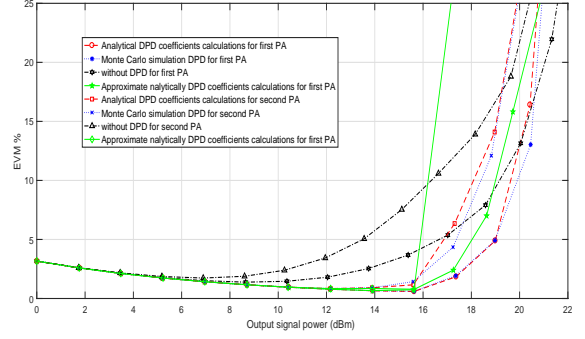
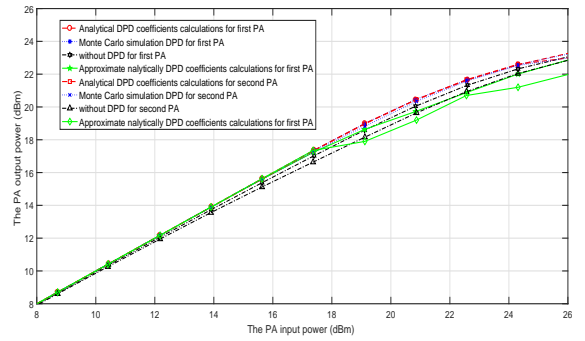
Figure 4. *EVM %* vs. output signal power in dBm for two PA's

Figure 5. Output power vs. Input power in dBm

the input power is less than 16 dBm:

$$\begin{aligned} A &= \sum_{k=0}^3 \alpha_k * a_{0,0}^{7-k} * a_{2,0}^k * \sigma^{2k} \\ B &= -a_{0,0}^4 a_{2,0} - 36 a_{0,0}^3 a_{2,0}^2 \sigma^2 - 504 a_{0,0}^2 a_{2,0}^3 \sigma^4 \\ C &= \sum_{k=0}^3 \gamma_k * a_{0,0}^{8-k} * a_{2,0}^k * \sigma^{2k} \end{aligned} \quad (18)$$

As shown in figure 4, When the signal power of the two PAs is less than 15.5 dBm the mathematical relationships of the DPD coefficients in equations (17) and (18) are represent a good approximate relationships for the first PA and second PA, respectively, Or in other words, the equation (18) is a good approximate equation for the two PAs or for any third order nonlinear PA with $a_{2,0} \leq |-0.8|$.

In four cases, PA only, DPD using Monte Carlo simulation followed by the PA, DPD based on the proposed exact analytical DPD coefficients estimation closed forms followed by the PA, and DPD based on the proposed approximate analytical DPD coefficients estimation closed forms followed by the PA, figure 5 depicts the output signal power versus the input OFDM signal power in dBm (AM/AM) for the two PAs assuming normalized gain. As input power increases (after 16 dBm) the neglected terms in equations (15), becomes dominant terms and the approximate relationships are not valid.

Table I

k	α_k	β_k	γ_k	η_k	ψ_k	τ_k	λ_k	ε_k	μ_k	ρ_k	σ_k	δ_k	ξ_k	k	σ_k	ξ_k
0	1	1	1	8	48	8	1	1	1	1	1	1	1	9	40	12
1	72	36	72	192	2304	144	72	48	24	3	6	9	5	10	40	3
2	2448	504	2520	2304	57600	1152	2520	1200	288	3	15	36	10	11	20	3
3	49920	3072	54528	15360	921600	3840	54528	19200	1920	1	20	84	10	12	4	9
4	648576	5760	778752	46080	9676800	-	778752	201600	5760	2	15	126	5	13	6	9
5	5253120	-	7326720	-	61931520	-	7326720	1290240	-	4	6	126	1	14	24	3
6	23592960	-	43084800	-	185794560	-	43084800	3870720	-	2	1	84	3	15	36	1
7	40919040	-	141557760	-	-	-	141557760	-	-	1	4	36	12	16	24	2
8	-	-	212336640	-	-	-	212336640	-	-	1	20	9	18	17	6	1

V. CONCLUSION

In this paper, the ILA is considered. We present an analytical method to estimate the DPD coefficients. We obtain a closed form expression for the proposed DPD algorithm, which is the first of its kind. Moreover, we took a case study at certain nonlinearity order and memory depth of the PA. The mathematical relationships of the DPD coefficients were induced. Furthermore, a performance comparison between the DPD based on the proposed analytical DPD coefficients estimation and the DPD based on Monte carlo simulations is obtained. Finally, we provided approximate relationships of the DPD coefficients closed form and these relationships were proven to be valid, through simulations, up to a certain input power.

APPENDIX

A. Appendix-A

From (7), $\mathbf{Y}^H \mathbf{Y}$ can be gotten:

$$\mathbf{Y}^H \mathbf{Y} = L \begin{bmatrix} h_{1,1} & h_{1,2} & \cdots & h_{1,K \times M} \\ h_{1,2}^* & h_{2,2} & \cdots & h_{2,K \times M} \\ \vdots & \vdots & \vdots & \vdots \\ h_{1,K \times M}^* & h_{2,K \times M}^* & \cdots & h_{K \times M, K \times M} \end{bmatrix}$$

where $h_{1,1}$, $h_{1,2}$, $h_{2,2}$, $h_{1,K \times M}$, $h_{2,K \times M}$, and $h_{K \times M, K \times M}$ are obtained in the following

$$h_{1,1} = |y[n]|^2 + \cdots + |y[n+L-1]|^2$$

Assuming large training symbols ($L \rightarrow \infty$), then $h_{1,1} = LE [|y|^2]$. Also,

$$h_{1,2} = y^*[n]y[n-1] + \cdots + y^*[n+L-1]y[n+L-2]$$

For a large training symbols ($L \rightarrow \infty$), then $h_{1,2} = LE [y^*[n]y[n-1]]$

$$h_{2,2} = |y[n-1]|^2 + \cdots + |y[n+L-2]|^2 = LE [|y|^2]$$

$$\begin{aligned} h_{1,K \times M} &= \sum_{t=0}^{L-1} y^*[n+t]y[n+t-(M-1)] \\ &|y[n+t-(M-1)]|^{K-1} = L \times \\ &E [y^*[n]y[n-(M-1)] |y[n-(M-1)]|^{K-1}] \end{aligned}$$

$$\begin{aligned} h_{2,K \times M} &= \sum_{t=0}^{L-1} y^*[n-1+t]y[n+t-(M-1)] \\ &|y[n+t-(M-1)]|^{K-1} = L \times \\ &E [y^*[n-1]y[n-(M-1)] |y[n-(M-1)]|^{K-1}] \end{aligned}$$

$$\begin{aligned} h_{K \times M, K \times M} &= \sum_{t=0}^{L-1} |y[n+t-(M-1)]|^{2K} \\ &= LE [|y|^{2K}] \end{aligned}$$

Therefore, equation (9) is obtained. The same thing for equation (10). By substituting in equation (10) from equation (6) and (7) and assuming the training symbols is large ($L \rightarrow \infty$), thus equation (10) is obtained

B. Appendix-B

From (2) substitute in (11), then y can be rewritten as

$$y = a_{2,0} u^3 + a_{2,0} u v^2 + a_{0,0} u j(a_{2,0} v^3 + a_{2,0} u^2 v + a_{0,0} v) \quad (19)$$

and $|y|^2$, $|y|^4$, and $|y|^6$ are obtained in the following equations:

$$|y|^2 = \sum_{i=0}^2 \sum_{l=0}^{3-i} \rho_{4i+l+1-\sum_{j=-1}^{i-1} j} a_{0,0}^i a_{2,0}^{2-i} u^{2(3-l-i)} v^{2l} \quad (20)$$

$$|y|^4 = \sum_{i=0}^4 \sum_{l=0}^{6-i} \sigma_{7i+l+1-\sum_{j=-1}^{i-1} j} a_{0,0}^i a_{2,0}^{4-i} u^{2(6-l-i)} v^{2l} \quad (21)$$

$$|y|^6 = \sum_{i=0}^6 \sum_{l=0}^{9-i} \delta_{10i+l+1-\sum_{j=-1}^{i-1} j} a_{0,0}^i a_{2,0}^{6-i} u^{2(9-l-i)} v^{2l} \quad (22)$$

where ρ_k , σ_k , and δ_k are tabulated in table I, II. Now, we define $z[n]$ as the postdistorter output and should be closest to the signal $x[n]$, so let's assume $z[n] = x[n]$,

$$z[n]y^*[n] = a_{0,0}(u^2 + v^2) + a_{2,0}(u^4 + 2u^2v^2 + v^4) \quad (23)$$

and $z[n]y^*[n] |y[n]|^2$ is as the following:

$$z[n]y^*[n] |y[n]|^2 = \sum_{i=0}^3 \sum_{l=0}^{5-i} \xi_{6i+l+1-\sum_{j=-1}^{i-1} j} a_{0,0}^i a_{2,0}^{3-i} u^{2(5-l-i)} v^{2l} \quad (24)$$

where ζ_k is tabulated in table I. Then, to obtain the expectation of $|y|^2$, $|y|^4$, $|y|^6$, $z[n]y^*[n]$, and $z[n]y^*[n] | y[n]|^2$ in order to substitute in equations (12) and (13) to get the DPD coefficients that in (8). As mentioned, u and v are two zero mean Gaussian random variables with variance σ^2 . For any non-negative integer P , the expected value of u^P or v^P are equal ($E(v^P) = E(u^P)$) and obtained in the following [22]:

$$E(u^P) = \begin{cases} 0 & \text{if } P \text{ is odd} \\ \sigma^P (P-1)!! & \text{if } P \text{ is even} \end{cases} \quad (25)$$

Here $n!!$ denotes the double factorial, that is, the product of all numbers from n to 1 that have the same parity as n . Thus, the mathematical expectation of $|y|^2$, $|y|^4$, $|y|^6$, $z[n]y^*[n]$, and $z[n]y^*[n] | y[n]|^2$ are obtained in the following:

$$E[|y|^2] = 2 a_{0,0}^2 \sigma^2 + 16 a_{0,0} a_{2,0} \sigma^4 + 48 a_{2,0}^2 \sigma^6 \quad (26)$$

$$E[z y^*] = 8 a_{2,0} \sigma^4 + 2 a_{0,0} \sigma^2 \quad (27)$$

$$E[|y|^4] = \sum_{k=0}^4 \eta_k a_{0,0}^{4-k} a_{2,0}^k \sigma^{4+2k} \quad (28)$$

$$E[|y|^6] = \sum_{k=0}^6 \psi_k a_{0,0}^{6-k} a_{2,0}^k \sigma^{6+2k} \quad (29)$$

$$E[z y^* | y|^2] = \sum_{k=0}^3 \tau_k a_{0,0}^{3-k} a_{2,0}^k \sigma^{4+2k} \quad (30)$$

where η'_k s, ψ'_k s, and τ'_k s are tabulated in the table I. Therefore,

$$[\mathbf{Y}^H \mathbf{Y}]^{-1} = \frac{1}{n} \begin{bmatrix} f & g \\ g & h \end{bmatrix}$$

where

$$\begin{aligned} n &= 16 \sum_{k=0}^8 \lambda_k a_{0,0}^{8-k} a_{2,0}^k \sigma^{6+2k} \\ f &= 24 \sigma^4 \sum_{k=0}^6 \varepsilon_k a_{0,0}^{6-k} a_{2,0}^k \sigma^{2k} \\ g &= 4 \sigma^2 \sum_{k=0}^4 \mu_k a_{0,0}^{4-k} a_{2,0}^k \sigma^{2k} \\ h &= a_{0,0}^2 + 8 a_{0,0} a_{2,0} \sigma^2 + 24 a_{2,0}^2 \sigma^4 \end{aligned} \quad (31)$$

where λ_k , ε_k , and μ_k are tabulated in table I. Thus, to get the DPD coefficients which obtained in (14), substitute in (8)

REFERENCES

[1] S. Parkvall, A. Furuskar, and E. Dahlman, "Evolution of LTE toward IMT-advanced," IEEE Communications Magazine, vol. 49, no. 2, pp. 84–91, February 2011.

[2] F. Boccardi, R. W. Heath, A. Lozano, T. L. Marzetta, and P. Popovski, "Five disruptive technology directions for 5G," IEEE Communications Magazine, vol. 52, no. 2, pp. 74–80, February 2014.

[3] E. Dahlman, S. Parkvall, and J. Skold, "5G NR, The Next Generation Wireless Access Technology," Academic Press, 2018.

Table II

k	δ_k	k	σ_k	δ_k	k	δ_k	k	δ_k	k	δ_k
9	1	18	4	6	27	20	36	150	45	1
10	6	19	12	15	28	120	37	150	46	3
11	48	20	12	105	29	300	38	75	47	3
12	168	21	4	315	30	400	39	15	48	1
13	336	22	1	525	31	300	40	6	49	–
14	420	23	2	525	32	120	41	24	50	–
15	336	24	1	315	33	20	42	36	51	–
16	168	25	–	105	34	15	43	24	52	–
17	48	26	–	15	35	75	44	6	53	–

[4] E. G. Larsson, O. Edfors, F. Tufvesson, and T. L. Marzetta, "Massive MIMO for next generation wireless systems," IEEE Commun. Mag., vol. 52, no. 2, pp. 186–195, February 2014.

[5] F. Rusek, D. Persson, B. K. Lau, E. G. Larsson, T. L. Marzetta, O. Edfors, and F. Tufvesson, "Scaling up MIMO: Opportunities and challenges with very large arrays," IEEE Signal Process. Mag., vol. 30, no. 1, pp. 40–60, Jan 2013.

[6] T. L. Marzetta, "Noncooperative cellular wireless with unlimited numbers of base station antennas," IEEE Trans. Wirel. Commun., vol. 9, no. 11, pp. 3590–3600, Nov. 2010.

[7] C. Park, L. Sundström, A. Wallen, and A. Khayrallah, "Carrier aggregation for LTE-advanced: Design challenges of terminals," IEEE Commun. Mag., pp. 76–84, Dec. 2013.

[8] Nokia, "R4-121205 Way forward for non-contiguous intraband transmitter aspects. Available at: <http://www.3gpp.org/>," Tech. Rep., 3GPP, Feb. 2013.

[9] A. Katz, J. Wood, and D. Chokola, "The Evolution of PA Linearization: From Classic Feedforward and Feedback Through Analog and Digital Predistortion," IEEE Microwave Magazine, vol. 17, no. 2, pp. 32–40, Feb 2016.

[10] P. Kenington, High-Linearity RF Amplifier Design. Boston: Artech House, 2000.

[11] F. M. Ghannouchi and O. Hammi, "Behavioral modeling and predistortion," IEEE Microwave Magazine, pp. 52–64, Dec. 2009.

[12] L. Ding, R. Raich, and G. Zhou, "A Hammerstein predistortion linearization design based on the indirect learning architecture," in 2002 IEEE International Conference on Acoustics, Speech and Signal Processing (ICASSP), pp. 2689–2692, November 2002.

[13] L. Ding, G. Zhou, D. Morgan, Z. Ma, J. Kenney, J. Kim, and C. Giardina, "A robust digital baseband predistorter constructed using memory polynomials," IEEE Transactions on Communications, vol. 52, no. 1, pp. 159–165, January 2004.

[14] C. Eun and E. Powers, "A new Volterra predistorter based on the indirect learning architecture," IEEE Transactions on Signal Processing, vol. 45, no. 1, pp. 223–227, January 1997.

[15] A. Zhu and T. Brazil, "An adaptive Volterra predistorter for the linearization of RF high power amplifiers," in IEEE MTT-S, pp. 461–464, June 2002.

[16] M. Schetzen, "Theory of pth-order inverses of nonlinear systems," IEEE Transactions on Circuits and Systems, vol. 23, no. 5, pp. 285–291, May 1976.

[17] M. Schetzen, The Volterra and Wiener Theories of Nonlinear Systems. New York: Wiley, 1980.

[18] D. Dardari, V. Tralli, and A. Vaccari, "A theoretical characterization of nonlinear distortion effects in OFDM systems," IEEE Trans. Commun., vol. 48, no. 10, pp. 1755–1764, 2000.

[19] H. Hemesi, A. Abdipour, and A. Mohammadi, "Analytical Modeling of MIMO-OFDM System in the Presence of Nonlinear Power Amplifier with Memory," IEEE Transactions on Communications, vol. 61, no. 1, January 2013, pp. 155–163.

[20] D. R. Morgan, Z. Ma, J. Kim, M. G. Zierdt, and J. Pastalan, "A Generalized Memory Polynomial Model for Digital Predistortion of RF Power Amplifiers," IEEE Transactions Signal Processing, vol. 54, no. 10, Oct. 2006, pp. 3852–3860.

[21] 3GPP Tech. Spec. 36.104, "LTE Evolved Universal Terrestrial Radio Access (E-UTRA) Base Station (BS) radio transmission and reception," v16.0.0 (Release 16), Jan. 2019.

[22] Papoulis, Athanasios, "Probability, Random Variables and Stochastic Processes," 4th Edition, p. 148.